Analysis of the Empirical Shell-Model Hamiltonian for "s-d shell" Nuclei

J. Borysowicz, W. Chung and B.H. Wildenthal

Various effective interactions have been proposed[1] for "s-d shell nuclei". Recently Chung has devised[2] a set of complete, empirical hamiltonians in the model space of d5/2, s1/2, d3/2 shell model orbits. The 3 single particle energies and 63 two-body matrix elements (2bme) of the hamiltonian were fit to the experimental energy levels in s-d shell. In the case of so-called "particle hamiltonian" 197 energy levels from A=17-24 nuclei were used in the fit.

We use three methods for analyzing the 2bme.

1) Straightforward tensor decomposition as described by Jensen and Harvey[3] and by Kirson.[4]
2) The method of projection or scalar product. In this method each part (that is triplet odd central, tensor even and so on) of a set of 63 2bme is assigned a numerical strength. The relative contributions of central, L·S, tensor, non-Gallilean and other parts of interaction are given in terms of this strength.
3) Fits to potential model with the simple radial forms.

In all three methods we estimate the uncertainties of a decomposition or of a fit using error matrix from the original fit of Chung.[2]

For the "particle interaction" of Chung[2] we have found that

1) ALS part of the interaction is important for quality of the fit to the experimental data. However, the matrix elements of ALS are small.
2) There is a strong evidence of non-central Gallilean forces in the interaction.
3) It is possible to find a good potential representation of the interaction. This potential gives ~0.35 MeV average deviation from the s-d shell energy levels as compared with 0.25 MeV deviation of the empirical fit.[2]

---

1. For the discussion of the effective interactions in s-d shell see ref. 2.
2. W. Chung, Ph.D. Thesis, Department of Physics, Michigan State University.
3. A.S. Jensen and M. Harvey, Canadian Journal of Physics, 49 (1971) 1837.
4. M. Kirson, Physics Let. 47B (1973) 110.

Renormalization of the Axial-Vector στ Matrix Element in sd Shell Beta-decay

B.A. Brown, W. Chung and B.H. Wildenthal

A fundamental problem in nuclear physics is to determine the effects of the nuclear medium on the free nucleon observables. One of the simpler non-trivial observables is the στ operator associated with the Gamow-Teller beta decay. Recently Wilkinson[1-3] made an extensive analysis of the experimental axial-vector beta decay of nuclei with $A \leq 22$ and found that in relationship to simple shell-model wave functions an average renormalization of -10.1±3.5% was needed to explain the data. As he pointed out in conclusion,[1] further progress could not be made until full shell-model wave functions were available allowing for the expansion of the total matrix element in terms of single-particle matrix elements. Several theoretical calculations have been made to try to account for this renormalization in terms of nuclear effects[4] and mesonic exchange effects.[5,6]

In this work we present a summary of an analysis of almost all experimentally observed Gamow-Teller beta decay strengths in the 1s-0d shell, $16<A<40$, using complete sd shell model wave functions. The results are unaffected by shell model truncations which might restrict the $d_{5/2}$-$d_{3/2}$ occupancy ratios to which the στ matrix elements are especially sensitive. We use the wave functions of Chung and Wildenthal[7] which were generated from empirical two-body interactions obtained from fits to energy levels and binding energies in the regions A=17-24 and A=32-39. The comparison of the calculated transition rates with the observed values alternately offers a test of the validity of the model and/or the specific Hamiltonians employed and a means of determining the need, if any, for a renormalization of the free-nucleon parameterization of the Gamow-Teller operator in this model space.

Following Wilkinson[2] the ft value is expressed as:

$$ft_{1/2}(1+\delta_R) = \frac{C}{B(F)+(g_A/g_V)^2 B(GT)} \qquad (1)$$

$$B(F) = \{T(T+1)-T_{3i}T_{3f}\}(1-\varepsilon)$$

$$B(GT) \equiv |\langle\sigma\tau\rangle|^2$$

$t_{1/2}$ is the partial half life, f is the integrated Fermi function and δ_R is the model independent outer radiative correction up to third order in the fine structure constant.[8] The constant C=6177±14 was chosen to reproduce the $0^+ \to 0^+$ Fermi transitions in the sd shell. ε is a correction due to the lack of isobaric symmetry for which we take an average theoretical value of $1-\varepsilon=0.995\pm0.003$ (Ref. 2). The free-nucleon value of $|g_A/g_V|=1.251\pm0.009$ is used from the neutron beta decay.[2]

Using Eq. 1 and the measured $t_{1/2}$ and Q value, $|\langle\sigma\tau\rangle|_{exp}$ was extracted for about 200 transitions in the sd shell. The shell model matrix elements for all of these except for a few nuclei in the middle of the shell were calculated and expanded in terms of the 5 single-particle matrix elements $\langle j|||\sigma\tau|||j'\rangle$ where 2j2j'=55,11,53 33 and 13. 54 transitions were selected on a strength criterion similar to Wilkinsen's to be fitted by the 5 single-particle matrix elements.

For orientation to the mass dependence of $\langle\sigma\tau\rangle$ and to the extent to which unrenormalized (bare) matrix elements alone can explain the data, the $\langle\sigma\tau\rangle$ matrix elements for mirror nuclei are shown in Fig. 1. The overall trend of the data (solid line) is followed very well by the bare shell-model prediction (dashed line).

The fitted single-particle matrix elements are given in Table I. The results are given for various mass regions including A=17 and A=39 alone for comparison. R is a reduction factor for the total matrix element defined as the average of $\langle\sigma\tau\rangle_{exp}/\langle\sigma\tau\rangle_{bare}$ for the region considered. σ is the rms value for $\langle\sigma\tau\rangle_{fitted}-\langle\sigma\tau\rangle_{exp}$. $\langle\sigma\tau\rangle_{bare}$ and $\langle\sigma\tau\rangle_{fitted}$ indicate the calculated matrix element using the bare and fitted single-particle matrix elements, respectively. All data was treated with equal weight in the fits because σ is many times larger than the experimental error which in many cases is as small as 1%. These values of σ mean that a residual variation of $\delta\langle\sigma\tau\rangle \simeq 0.04$ cannot be accounted for by the present model which indicates that many-body effects in the wave function and/or the operator contribute to this extent.

The best $d_{5/2}$-$d_{5/2}$ matrix element for the region 17-23 is only 3% different than the A=17 value while the best $d_{3/2}$-$d_{3/2}$ matrix element for the region 33-39 is 9% different than the A=39 value. This indicates that deformed state admixtures have a greater effect in A=39 than in A=17.

The fit including the ℓ-forbidden $s_{1/2}$-$d_{3/2}$ matrix element gives a very small value consistent with zero. The $s_{1/2}$-$s_{1/2}$ and $d_{5/2}$-$d_{3/2}$ matrix elements are nearly the same for all A, and require reductions of (A=17-39) -19% and -31%, respectively. This is the first time that these empirical single-particle matrix elements have been obtained.

It is interesting to note that in the region A=25-33 that all of the single-particle matrix elements each require a much larger reduction than the average reduction R. This is due to the state dependence of the single-particle reduction factors combined with a cancellation between single-particle matrix elements in the total matrix element. For A=17-23 the reduction factor R is the same as than obtained by Wilkinson.[2]

These results are being compared with recent theoretical calculations for the $d_{5/2}$-$d_{5/2}$ and

$d_{3/2}$-$d_{3/2}$ matrix elements.[4-6] It would be very important to have similar calculations for the other three single-particle matrix we have obtained.

1. D.H. Wilkinson, Nucl. Phys. A225, 365(1974).
2. D.H. Wilkinson, Nucl. Phys. A209, 470(1973).
3. D.H. Wilkinson, Phys. Rev. C7, 930(1973).
4. K. Shimizu, M. Ichimura and A. Arima, Nucl. Phys. A226, 282(1974).
5. M. Rho, Nucl. Phys. A231, 493(1974).
6. A. Barroso and R.J. Blin-Stoyle, Nucl. Phys. A251, 446(1975).
7. W. Chung and B.H. Wildenthal, to be published; W. Chung thesis, Michigan State University.
8. Computer programs for f and δ_R were obtained from R. Firestone.

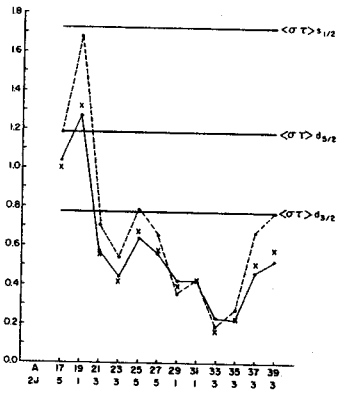

FIG. 1.--The $|\langle\sigma\tau\rangle|$ matrix elements for mirror nuclei. The solid line connects experimental points (which have small error bars). The dashed lines connect the shell model results using bare single-particle matrix elements. The crosses are the shell model results using fitted single-particle matrix elements obtained from a fit to 54 data between A=17 and A=39.

Table I. Results of the present analysis.

Bare Single Particle Values				$\langle j\|\|\|\sigma\tau\|\|\|j'\rangle$				
				2j2j' = 55	11	53	33	13
				7.10	6.00	-7.59	-3.80	0
Mass Region	Number of Data	R[a]	σ[b]					
17	1	0.878		6.23(5)[c]				
39	1	0.675					-2.56(3)[c]	
17-39	54	0.89	0.042	5.99(8)[d]	4.88(12)	-5.27(11)	-2.82(11)	[0][e]
17-39	54	0.89	0.041	6.01(8)	4.86(12)	-5.25(11)	-2.83(11)	-0.12(12)
18-38	52	0.89	0.041	5.96(9)	4.87(12)	-5.27(11)	-2.92(12)	[0]
17-23	23	0.88	0.048	6.04(12)	4.40(33)	-5.45(18)	[-2.56]	[0]
25-33	18	0.92	0.024	5.76(9)	4.87(8)	-5.29(12)	-3.21(14)	[0]
33-39	16	0.82	0.035	[5.99]	4.72(24)	-5.33(18)	-2.80(9)	[0]

a) R is the average reduction factor for the total matrix element; $\langle\sigma\tau\rangle_{exp}$ /$\langle\sigma\tau\rangle_{bare}$
b) σ is the rms value of $\langle\sigma\tau\rangle_{fitted}$ - $\langle\sigma\tau\rangle_{exp}$
c) Experimental error only
d) Fit error only
e) []indicates a fixed parameter.

Renormalization of Two-Nucleon Transfer Strengths in Small Model Space Shell-Model Calculations

B.A. Brown

It is well known that the absolute magnitude of the cross section for two-nucleon transfer is underestimated by one to two orders of magnitude if wave functions with only a few shell model components are used to describe the states involved. Part of the enhancement which will be denoted by D_0^2 originates from approximations made in the DWBA analysis[1] (such as zero range). Another source of enhancement, which will be denoted by ϵ, comes from nuclear correlation effects. This two-particle correlation can be found in the shell model if a large number of single-particle orbitals, at least all the orbitals in a major shell, are coherently mixed via a short-range attractive interaction.[2,3] However, such large shell model calculations are possible only in the simplest cases, and for nuclei with many valence particles approximations must be made.

It was pointed out many years ago that for nuclei in the $f_{7/2}$ shell the relative $0^+ \to 0^+$ (p,t) and (t,p) strengths are fairly well reproduced with $f_{7/2}$ wave functions.[4,5] In an analysis of recent (p,t) experiments[6-8] using $f_{7/2}$ wave functions it was found that the relative strengths throughout the $f_{7/2}$ shell for all transfers of a given J in (p,t) are well reproduced by the $f_{7/2}$ model but that the enhancement factors are very J dependent.

In the present work, we investigate how this J-dependent but state and nucleus independent enhancement can be understood. The situation for the ^{54}Fe(p,t)^{52}Fe reaction is illustrated diagrammatically in Fig. 1. Fig. 1a shows the zeroth-order process, which is the result of the two-neutron annihilation operator acting on an initial state with a filled $f_{7/2}$ neutron shell. The admixture of other orbits is then considered in perturbation theory. Figure 1b represents the effect of the admixture of two neutron holes below the $f_{7/2}$ shell in the final state and Fig. 1c represents the admixture of two neutron particles above the $f_{7/2}$ shell in the initial state.

For the reaction $J_i \overset{J}{\to} J_f$ where J is the transferred angular momentum (J=L for S=0), the zeroth order process has a cross section proportional to:

$$A_J(f_{7/2}^2)\langle \mathrm{DWBA}(f_{7/2}^2)\rangle_J \qquad (1)$$

where $C^2S(f_{7/2}^2)=A_J^2(f_{7/2}^2)$ and $\sigma_{\mathrm{DWBA}}(f_{7/2}^2)=|\langle \mathrm{DWBA}(f_{7/2}^2)\rangle_J|^2$. Whereas the first-order processes have a cross section proportional to:

$$\frac{-A_J(f_{7/2}^2)\langle f_{7/2}^2 J|V|j'j''J\rangle\langle \mathrm{DWBA}(j'j'')\rangle_J}{|E(j')+E(j'')-2E(f_{7/2})|} \qquad (2)$$

where j' and j" are all of the orbitals above and below the $f_{7/2}$ shell which can couple to the transferred angular momentum J; E are the single-particle energies. Combining Eqs. 1 and 2, an enhancement factor ϵ_J can be defined as

$$\epsilon_J=\left(1+\sum_{j',j''\neq j}\delta_J(j'j'')\right)^2 \qquad (3)$$

$$\delta_J(j'j'')=\frac{-\langle j^2 J|V|j'j''J\rangle\langle \mathrm{DWBA}(j'j'')\rangle_J}{|E(j')+E(j'')-2E(j)|\langle \mathrm{DWBA}(j^2)\rangle_J}$$

where $j=f_{7/2}$ in this case. This enhancement factor fulfills the required properties that it depend on J but not on J_i or J_f or on the specific nuclei. It is a consequence of the fact that only admixtures with two particles above or two holes below the $f_{7/2}$ shell are allowed. Eq. 3 is only a good approximation when the DWBA angular distributions do not depend strongly on the particular orbitals involved as is usually the case for (p,t) reactions. <DWBA> is most easily used as the differential cross section integrated over the angular range observed in the experiment.

There are many higher order diagrams such as the one shown in Fig. 1d which are much more complicated, but hopefully these are not as important. In addition, for the (t,p) reaction to excited states with J≠0, direct population of states with only one particle above the $f_{7/2}$ shell is possible which can lead to a state and nucleus dependent enhancement factor.

Using a delta-function interaction and the zero-range DWBA code DWUCK, ϵ_J were calculated for the ^{54}Fe(p,t)^{52}Fe reaction.[6] Single-particle energies were taken from Ref. 9. The results are given in Table I and compared with the experimental enhancements ϵD_0^2 by extracting a D_0^2 for each J. $\delta_J(j'j'')$ turns out to be positive for all j'j" and hence the sum in Eq. 3 is very coherent. This simple calculation seems to nicely account for most of the observed J-dependence leaving a $D_0^2 \simeq 40$ which is close to the value needed in the sd shell using complete sd shell wave function, $D_0^2 \simeq 33$ (Ref. 10).

Plans are to extend these calculations to pn transfer for odd J and to study the (presumably small) single-particle and Q-value dependence in Eq. 3. A similar analysis of the three and four nucleon transfer may be feasible.

1. H.W. Baer et al., Annals of Physics 76, 437(1973).
2. R.H. Ibarra et al., Nucl. Phys. A241, 189 (1971).
3. R.A. Broglia et al., Nucl. Phys. A169, 225(1971).
4. R.F. Casten et al., Phys. Rev. C4, 130(1971).
5. G. Bassani et al., Phys. Rev. 136, B1006 (1964).
6. P. Decowski et al., to be published.
7. A. Saha et al., to be published, and A. Saha,Thesis, Northwestern University (1977).
8. G. Crawley et al., Phys. Rev. C8, 574(1973).
9. M. Harvey et al., Nucl. Phys. A221, 77(1974).
10. H. Nann et al., Phys. Rev. C13, 1009(1976).

TABLE I.--Normalization factors needed in the DWBA analysis of the ^{54}Fe(p,t) data (Ref. 6) and calculated enhancement factors.

J	ϵD_0^2 [a] exp	(fp) orbitals ϵ(th)	(fp) orbitals D_0^2	(sd-fp-$g_{9/2}$) orbitals ϵ(th)	(sd-fp-$g_{9/2}$) orbitals D_0^2
0^+	189	2.16	86	4.33	42
2^+	89	1.49	60	2.26	38
4^+	45	1.10	40	1.32	32
6^+	20(32[b])	1.00	20(32[b])	1.03	20(32[b])

[a] In units of 10^4 MeV^2-fm^3. These strengths are those the 45 MeV data of Ref. 6 multiplied by a factor of 2.03 in order to reproduce the absolute cross sections of the E_p=40 MeV data of Ref. 5.

[b] Experimental and DWBA cross sections corresponding to the L=6 cross sections at 30°, other numbers are for cross sections integrated between 6° and 60°.

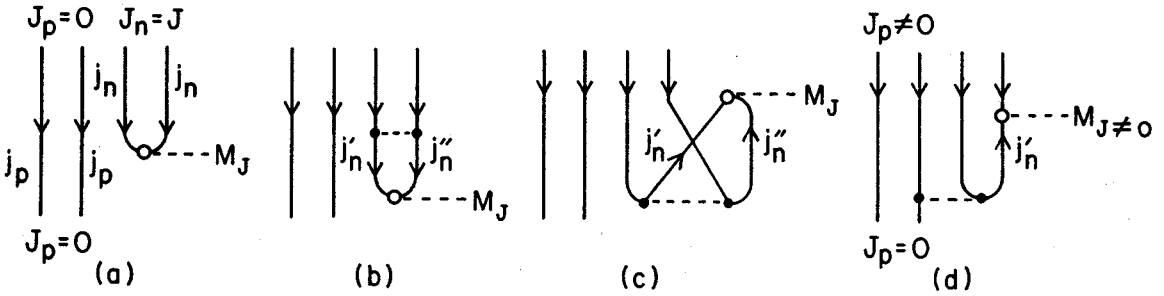

Spectroscopic Amplitudes for Multi-nucleon Transfer in the $1f_{7/2}$ Shell

B.A. Brown

The $f_{7/2}$ shell model[1,2] has been found to provide a coherent description of many properties of a subset of energy levels in nuclei with $20<N<28$ and $20<Z<28$. In this work the success of this model in describing multi-nucleon transfer spectroscopic amplitudes is investigated. It is known that the $f_{7/2}$ model cannot account for the absolute magnitude for two-nucleon transfer because admixtures of nearby "hot" orbitals greatly enhance the cross section.[3] However, the $f_{7/2}$ model could be considered successful if at least relative spectroscopic factors can be predicted; this is similar to the effective charge concept for electromagnetic transitions.[4]

The wave functions are conveniently described in the proton-neutron formalism, for example

$$|J_i> = \sum_{J_{pi}J_{ni}} (a^{J_i}_{J_{pi}J_{ni}}) |(J_{pi},J_{ni})J_i>$$

where the J's stand for all indicies needed to distinguish the states. Then the most general spectroscopic amplitude for the transfer of p protons and n neutrons in the configuration $(J_p,J_n)J$ is,

$$A(p,n,J_p,J_n,J)J_i \leftrightarrow J_f$$
$$= \sum_{J_{pi},J_{ni},J_{pf},J_{nf}} (a^{J_i}_{J_{pi},J_{ni}})(a^{J_f}_{J_{pf},J_{nf}})((^{n_i}_{n})(^{p_i}_{p}))^{1/2}$$
$$\times (j^{p_i-p}(J_{pf})\, j^{p}(J_p)\,|\}\, j^{p_i}(J_{pi}))$$
$$\times (j^{n_i-n}(J_{nf})\, j^{n}(J_n)\,|\}\, j^{n_i}(J_{ni}))$$
$$\times \begin{Bmatrix} J_{pi} & J_p & J_{pf} \\ J_{ni} & J_n & J_{nf} \\ J_i & J & J_f \end{Bmatrix}$$

$(|\})$ are multi-particle cfp for identical particles. The relation to the one-nucleon spectroscopic factor is $C^2S=A^2(J=j)J_i \leftrightarrow J_f$.

For two-nucleon transfer J_p and J_n are unique for a given J and the amplitudes are combined with a DWBA analysis to calculate absolute cross sections. DWBA codes for microscopic three and four nucleon transfer are not yet available and thus only relative cross sections have been calculated by combining the spectroscopic amplitudes with the "G" factors for three nucleon transfer (Ref. 5) or four nucleon transfer (Ref. 6).

$$\sigma \propto \Big(\sum_{J_pJ_n} A(p,n,J_pJ_n,J)G(J_p,J_n,J) \Big)^2$$

(p,t) Reactions

A numer of high resolution (p,t) experiments have recently been carried out[7-9] which has allowed the identification of states for all L transfers ($L=J_n=J$) up to the maximum L=6. The data has been analyzed using the zero-range DWBA code DWUCK[10] with the optical model parameters of Ref. 11

$$\sigma_{th} = 9.72\, A^2(J)\sigma_{DWUCK}\epsilon D_0^2 (2J+1)^{-1}$$

ϵD_0^2 is treated as an empirical normalization factor to be determined by a comparison of experiment with theory. The average ϵD_0^2 for several (p,t) reactions are given in Table I. ϵD_0^2 is found to be strongly J dependent but nearly independent of J_i, J_f and the specific nuclei. Once the J-dependent ϵD_0^2 are chosen, the comparison with experiment is excellent for levels of the same isospin in even-even and odd-even nuclei (Table II) as well as levels with different isospins in the same nucleus (Table III).

TABLE I.--J-dependent enhancement factors obtained from a comparison of experimental and theoretical integrated cross sections for (p,t) reactions.

Reaction	Ref.	E_p (MeV)	$f_{7/2}$ Int[a]	ϵD_o^2 (10^4 MeV^2-fm^3) J=0	2	4	6
^{44}Ca(p,t)	9	39	^{42}Sc	171	106	46	20
^{48}Ca(p,t)	7	40	^{48}Sc	171	71	36	16
^{50}Ti(p,t)	9	40	^{48}Sc	152	63	25	15
			^{48}Sc*	157	65	25	16
^{54}Fe(p,t)	8	45	^{54}Co	93	44	22	10(16[c])
^{54}Fe(p,t)	8[b]	40	^{54}Co	189	89	45	20(32[c])

[a] The $f_{7/2}$ two-body interactions from Ref. 2 were used to obtain the $f_{7/2}$ wave functions; ^{48}Sc* is discussed in the text.
[b] These strengths are those of the E_p=45 MeV data of Ref. 8 multiplied by 2.03 in order to reproduce the absolute cross sections of the E_p=40 MeV data of Ref. 19.
[c] Experimental and DWBA cross sections corresponding to the L=6 cross sections at 30°, other numbers are for integrated cross sections.

The angular distributions are fit relatively well by the DWBA except for J=6.[7,8] This leads to a large difference in the exp-th comparison for J=6 depending on if they are normalized at the maximum in the angular distribution or if they are normalized by the integrated cross sections as illustrated in Table I for the ^{54}Fe(p,t) analysis.

In general the spectroscopic amplitudes are fairly independent of the $f_{7/2}$ two-body interaction. However, in the case of ^{48}Ti if the effective interactions V_{pp}, V_{pn}, and V_{nn} are all equal for T=1, mixing between states is limited by the signature selection rules.[12] The interaction ^{48}Sc*, where $V_{pp}=^{50}$Ti, $V_{pn}=^{48}$Sc, and $V_{nn}=^{46}$Ca (levels in ^{46}Ca), causes signature mixing and results in (p,t) amplitudes which are in better agreement with experiment (see Table II).

TABLE II.--Comparison of experimental[9] and theoretical cross sections integrated between 6° and 55° for the ^{50}Ti(p,t) and ^{51}V(p,t) reactions with E_p=40 MeV using ϵD_0^2 from Table I.

J_f	Exp		Th(^{48}Sc)	Th(^{48}Sc*)	
	Energy keV	σ μb	σ μb	σ μb	Energy keV
^{48}Ti(π=+)					
0	0	42.2	42.2	42.2	0
2	985	21.1	18.1	21.1	1110
2	2416	9.4	12.5	9.4	1963
4	2295	4.47	5.51	5.93	2254
4	3238	9.58	8.54	8.06	3088
6	3333	6.26	4.13	6.44	3018
6	3511	2.90	5.00	2.75	3231
^{49}V(π=-)					
3/2	153	1.16	1.17	1.08	666
3/2	1662	1.19	1.64	1.82	2085
5/2	91	1.28	1.17	1.30	118
5/2	1516	2.45	2.26	2.23	1650
7/2	0	36.6[a]	37.0[a]	35.5[a]	0
7/2	2183	5.0[b]	4.5[b]	4.4[b]	2379
9/2	1154	5.5	3.0	3.0	1391
9/2	2350	1.4	3.2	3.5	1961
11/2	1020	6.08	5.90	6.61	1051
13/2	2861	2.02	1.48	1.42	2972
15/2	2263	1.17	1.34	1.56	2244

[a] Mostly L=0

[b] Mostly L=2

TABLE III.--Comparison of experimental[8] and theoretical cross sections integrated between 6° and 60° for the ^{54}Fe(p,t) reaction with E_p=45 MeV using ϵD_0^2 from Table I.

J_f	T_f	Exp		Th(^{54}Co)		
		Energy keV	σ μb	σ μb	C^2S L=J_f	Energy keV
^{52}Fe(π=+)						
0	0	0	13.4	14.7	0.558	0
0	2	8561	7.3	7.3	0.250	8055
2	0	850	6.0	7.7	1.77	1049
2	1	6034	6.5	6.5	1.72	5512
2	1	6044				
2	2	10006	1.4	1.4	0.42	9501
4	0	2385	2.8	2.8	1.88	2726
4	0	3583				
4	1	6416	4.7	4.7	3.84	6065
4	2				0.75	10685
6	0	4326	1.0	1.3	2.69	4327
6	0	4869				
6	1	5652	1.6	1.6	3.73	5216
6	2				1.08	11140
all J_f=0					1	
all J_f=2					5	
all J_f=4					9	
all J_f=6					13	

(p,^{3}He) Reactions

Several high resolution (p,^{3}He) experiments leading to odd-odd nuclei were carried out by Guichard *et al.*[13] Sum rule spectroscopic factors were used by them for the interpretation; however, in the present calculation the spectroscopic strength is usually found to be split among several low lying states as well as states with higher isospin. For the ^{52}Mn(p,^{3}He) reaction a ratio of $R=\{D(S=1)/D(S=0)\}^2=0.45$ was extracted from the DWUCK analyses of the 870 keV 7^+(L=6,S=1) and g.s. 6^+(L=6,S=0) strengths. Values of R in the sd shell range from 0.3 to 0.4 (Ref. 14). For the ^{52}Mn(p,^{3}He) reaction the enhancement factors for odd J fall smoothly in between the enhancement factors for even J given in Table I.

(t,p) and (^{3}He,n) Reactions

In most of these experiments on even-even nuclei only the $0^+\rightarrow0^+$ and $0^+\rightarrow2^+$ transitions are resolved. The calculated $0^+\rightarrow2^+$ spectroscopic amplitudes decrease sharply with increasing mass. The experimental $0^+\rightarrow2^+$ strengths also decrease with mass but not nearly as fast.[15] This failure of the $f_{7/2}$ model to explain even the relative $0^+\rightarrow2^+$ strengths is probably due to admixtures of configurations with one particle in an orbit above the $f_{7/2}$.

(p,α) and (α,p) Reactions

The ^{40,42,44}Ca, ^{48}Ti(α,p) g.s.→g.s. relative cross sections for J=7/2 are well reproduced by the $f_{7/2}$ model except for some enahncement in the ^{40}Ca(α,p) cross section.[16] The ^{45}Sc(α,p)^{48}Ti experiment was recently carried out;[17] the cross sections to the $J_f=0^+,2^+,4^+$ and 6^+ states in ^{48}Ti are spectroscopically dominated by J=7/2 and J_n=0 even though many other J and J_n are possible. The calculated cross sections are in good agreement with experiment. The ^{52}Cr(p,α)^{49}V reaction is interesting because many high-spin non yrast levels are predicted to be strongly populated. For example, the strongest $J_f=15/2^-$ level is the third one calculated to lie at 3585 keV. A state observed strongly at 3612 keV (Ref. 5) is a good candidate for this $15/2^-$ level.

(^{6}Li,d) Reactions

α transfer spectroscopic amplitudes were calculated for the (^{6}Li,d) reactions carried out by the Rochester group.[18] Relative spectroscopic factors are compared in Table IV. The ^{40}Ca(^{6}Li,d) $0^+\rightarrow0^+$ transition is enhanced. A similar but smaller enhancement was observed in the ^{40}Ca(α,p) $0^+\rightarrow7/2^-$ transition but not in the ^{40}Ca(t,p) or ^{40}Ca(^{3}He,n)$0^+\rightarrow0^+$ transitions. This indicates that a T=0 proton-neutron correlation may be needed to explain this enhancement. The most serious exp-th discrepancy is the 2^+ to g.s. ratio in ^{50}Cr(^{6}Li,d). This seems to be related to the problem of the $0^+\rightarrow2^+$ enhancement in (t,p) and (^{3}He,n) discussed above.

Table IV--Comparison of experimental[18] and theoretical spectroscopic factors for (^{6}Li,d) reactions.

Target Nucleus	S(g.s.) exp	S(g.s.) th	S(2^+)/S(g.s.) exp	S(2^+)/S(g.s.) th	S(4^+)/S(g.s.) exp	S(4^+)/S(g.s.) th
^{40}Ca	2.9	0.95	2.0	1.44	4.8	4.7
^{42}Ca	1.19	1.07	1.15	1.13	2.1	0.91
^{44}Ca	1	1	1	1	1	1
^{50}Cr	0.3	1.07	0.7	0.05		0.44

The $f_{7/2}$ model probably provides a much better description of the (d,^{6}Li) reaction, but these experiments have not been done.

1. J.D. McCullen, B.F. Bayman and L. Zamick, Phys. Rev. 134, B515(1964).
2. W. Kutschera, B.A. Brown and K. Ogawa, submitted to Rivista del Nuovo Cimento.
3. B.F. Bayman and N.M. Hintz, Phys. Rev. 172, 1113(1968).
4. B.A. Brown et al., Phys. Rev. C9, 1033(1974).
5. P. Smith, Thesis, Michigan State University (1976) and private communication.
6. D. Kurath and J.S. Towner, Nucl. Phys. A222, 1(1974).
7. G. Crawley et al., Phys. Rev. C8, 574(1973).
8. P. Decowski et al., to be published.
9. A. Saha, Thesis, Northwestern University (1977); A. Saha, H. Nann and K.K. Seth, to be published.
10. H.W. Bear et al., Annals of Physics 76, 437(1973).
11. H. Nann and B.H. Wildenthal, Phys. Rev. C13, 1009(1976).
12. R.D. Lawson, Nucl. Phys. A173, 17(1971).
13. A. Guichard et al., Phys. Rev. C12, 540(1976); Phys. Rev. C12, 1780(1975) and references therein.
14. D.G. Fleming et al., Nucl. Phys. A162, 225(1971).
15. D. Evers et al., Nucl. Phys. A230, 109(1974) and private communication.
16. R.O. Ginaven and A.M. Bernstein, Nucl. Phys. A154, 417(1970).
17. P. Smith, private communication.
18. H.W. Fulbright et al., Nucl. Phys. A284, 329(1977).
19. G. Bassani et al., Phys. Rev. 136, B1006 (1964).

Coulomb Displacement Energies in the $1f_{7/2}$ Shell

B.A. Brown and R. Sherr*

The displacement energies of neighboring analogue states provide an important test of the nuclear interactions. If we assume that the strong interaction is the same for the n-n n-p and p-p T=1 interactions then the displacement energies give direct information on the many-body structure of the nuclear wave functions since the Coulomb interaction is well known. Alternatively, if the nuclear structure is known then the displacement energies provide information on the T_z dependence of the strong interaction. The total displacement energy will depend on both of these effects. Most of the theoretical effort has been expended on the nuclei plus or minus one nucleon from the closed shells since the nuclear structure is presumably simplest in these cases.

Recently the multiparticle shell model has been used to explain the displacement energies of all levels with a particular j^n configuration[1-3] for all analogue pairs which include among others isobaric quartets and mirror nuclei. Most of the calculations have been limited to the generalized seniority scheme[4] for pure j^n configurations such as $d^n_{3/2}$ or $f^n_{7/2}$. These calculations in their simplest form are limited by the assumption that the two-body matrix elements are independent of J for $J\geq 2$. Nevertheless the fits to experiment have been very good.[1-3] In these fits all of the displacement within a shell are found to be related to a one-body term C plus a two-body charge asymmetric interaction $V\equiv V_{pp}-V_{nn}$ and a two-body charge dependent interaction $d\equiv V_{pn}-V_{nn}$. In the generalized seniority scheme at most four quantities are obtained V_0, d_0, $\bar{V}_2$ and $\bar{d}_2$. Where V_0 and d_0 are the interactions in the j^2 J=0 state and $\bar{V}_2$ and $\bar{d}_2$ are the (2J+1) weighted average of all states with $J\geq 2$. The scope of previous exact shell model calculations[5-9] which are not limited to generalized seniority have been very limited either in the number of nuclei and states considered (refs. 6-9) or in the number of parameters allowed (ref.5)

In the present work we report on a shell model calculation for the displacement energies in the $f_{7/2}$ shell for A=41-55. The displacement energies are written in perturbation theory as:

$$\Delta E = \left(\frac{A_o}{A}\right)^{\lambda/3} (C + \sum_J p_J V_J + \sum_J q_J d_J)$$

where A_o=40 and where C, V and d are assumed to have fixed values. The coefficients p and q are obtained from the shell model wave functions which have good isospin; p and q are different for every analogue pair. The coefficients p and q are not very sensitive to the different empirical interactions considered by Kutschera et al,[10]; in the present calculation the ^{42}Sc interaction was used.

The nuclear size dependence λ has been discussed in ref. 3 where it was found that the values of λ, C, V and d are very correlated in a χ^2 search. In the present report we take λ=0.2, a value which is obtained by assuming that the A=55 displacement energy has the correct ratio of core (^{40}Ca) to valence ($1f_{7/2}$) contribution when compared with the A=41 displacement energy which only has a core contribution. This ratio for A=55 is ≃20/7 and is equal to 3.06 if harmonic oscillator wave functions are used. This value of λ is close to the shallow minimum obtained in a χ^2 search,[3] but the final result depends on the above assumption. The variation of the parameters V and d with λ is shown in ref. 3.

For cases in which the wave functions are unique such as the ones in which one of the nuclei lies on Z=20 or N=28 the present calculation is the same as previous calculations[2,3] and the results are necessarily the same except for the λ dependence. For most levels the present results are very similar to the generalized seniority model. The most important differences arise from the J-dependence in V_J and d_J for $J\geq 2$.

In the present work about 50 displacement energies from A=41-55 were fitted with the 7 quantities C, V_0, V_2, V_4, V_6, d_0 and $\bar{d}_2$. No improvements could be made by allowing d_2, d_4 and d_6 to vary separately. The results for a fit to 42 displacement energies between A=43 and 55 are shown in the figure and listed in Table I. V_J and d_J obtained from individual levels in A=42 are also shown in the figure.

The most interesting results for A=43-55 are that $V_0 \simeq V_2 \simeq 400$ keV and that $d_0 \simeq -50$ keV. These same features (but different values) are observed in A=42 but have not been previously studied seriously because of the well known problems with core excited states in these nuclei. We see that these are actually very general features for which an explanation is needed. In zeroth order V_J are just the two particle Coulomb energies. A typical calculation[6] for the Coulomb interaction is shown in the figure. The calculation resembles very little the empirical matrix elements V_J which indicates that nuclear polarization effects and/or a charge asymmetric strong interaction are important. The Coulomb interaction does not contribute in zeroth order to d_J, hence the negative empirical value for d_0 is again evidence for a higher order effect. It is interesting that the quantity V-2d (shown in the figure) most closely resembles the pure Coulomb interaction.

TABLE I.--Parameters obtained from fit to displacement energies from A=41-55 excluding A=42.

Parameter	value
λ[a]	0.2
C	7299 keV
V_0	402 keV
V_2	407 keV
V_4	337 keV
V_6	305 keV
d_0	-47 keV
$\bar{d}_2$	-3 keV

[a] Fixed parameter.

(Note that V-2d is the experimental quantity shown by Bertsch.[6])

The fit for A=43-55 resulted in an rms experimental-theoretical difference of 12.3 keV compared with the rms experimental error of 11.7 keV. The fit was carried out with equal weight for all data in which the experimental error did not exceed 25 keV. For two cases the fitted displacement energies were many standard deviations away from the experimental errors and hence these were excluded from the fit. These were the following nuclei(exp value/fitted value)

^{46}Sc - ^{46}Ca J=0 T=3 7167±4/7195,

^{50}Mn - ^{50}Cr J=0 T=2 8412±2/8431.

Experiments are currently being carried out to check some of these discrepancies.[17] If the fit is extended from A=43-55 to A=42-55 then the experimental-theoretical rms increases from 12.3 to 16.5 indicating that A=42 is somewhat special presumably because of admixtures with low lying 4p-2h core excitations.

Even though a pure $f^n_{7/2}$ model was used successfully to extract values of V_J and d_J which can explain displacement energies in the $f_{7/2}$ shell, V_J and d_J must be regarded as effective matrix elements which include admixtures from other orbitals. They are no different than any other one and two body operators within truncated shell-model calculations in this regard. These admixtures include all $0\hbar\omega$ fp orbitals as discussed by Bertsch[6] and Shlomo[7] as well as $1\hbar\omega$ and $2\hbar\omega$ excitations which include the collective monopole and quadrupole states among others. The $1\hbar\omega$ and $2\hbar\omega$ core polarization contributions to the T=1/2 mirror displacement energies have been discussed extensively in the literature (most recently in refs. 11-13) in an unsuccessful attempt to explain the Nolen-Schiffer anomaly[14] with a charge symmetric nucleon-nucleon interaction. This failure has lead to the suggestion that a charge asymmetric strong interaction is responsible.[15,16] Perhaps a detailed study of the $1\hbar\omega$ and $2\hbar\omega$ contributions in the $1f_{7/2}$ shell similar to the analysis carried out by Kahana[9] for A=18 can shed additional light on the importance of the charge asymmetric as well as the charge dependent strong interactions.

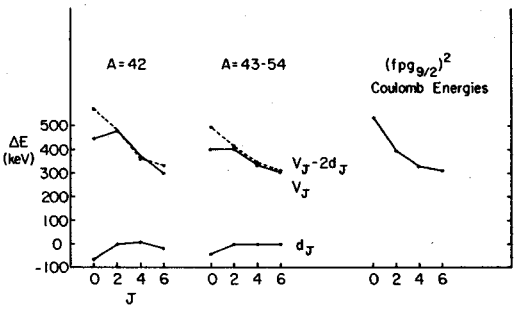

*Princeton University.

1. R. Sherr and I. Talmi, Phys. Letts. 56B,212 (1975).
2. J.M.G. Gomez, Phys. Letts. 62B,25(1976).
3. R. Sherr, Phys. Rev. C, to be published.
4. K.T. Heckt, Isobaric Spin in Nuclear Physics, ed. by J.D. Fox and D. Robson (Academic Press, N.Y. 1966) p. 823; Nucl. Phys. A102, 11(1967); Nucl. Phys. A114,280(1968).
5. R.R. Whitehead, A. Watt, D. Kelvin and H.J. Rutherford, Phys. Letts. 65B,323(1976).
6. G.F. Bertsch, Phys. Rev. C174,1313(1968).
7. S. Shlomo and G.F. Bertsch, Phys. Letts. 49B,401(1974).
8. E.H. Auerbach, S. Kahana, C.K. Scott and J. Weneser, Phys. Rev. C188,1747(1969).
9. S. Kahana, Phys. Rev. C5,63(1972).
10. W. Kutschera, B.A. Brown and K. Ogawa, to be published in Rivista del Nuovo Cimento.
11. A. Barroso, Nucl. Phys. A281,267(1977).
12. N. Auerbach, Nucl. Phys. A229,447(1974).
13. W.G. Love and S. Shlomo, preprint.
14. J.A. Nolen and J.P. Schiffer, Ann. Rev. Nucl. Sci. 19,471(1969).
15. H. Sato, preprint.
16. J.W. Negele, Nucl. Phys. A165,305(1971).
17. R. Kouzes, P. Kutt, D. Mueller and R. Sherr, Princeton University, (unpublished).

Empirical Single-Particle $\langle r^2 \rangle$ Matrix Elements Deduced from Rms Charge Radii and E0 Transitions in the sd Shell

B.A. Brown, W. Chung and Jan van Hienen

In the harmonic oscillator model all of the $\langle j|r^2|j\rangle$ matrix elements within the sd shell are the same size independnet of j. However, such things as small single-particle binding energies and E0 core polarization can give rise to an orbital dependence. The E0 core polarization is particularly interesting because it is very sensitive to the nuclear interaction. For example, density independent and density dependent interactions give opposite signs for the E0 core polarization.[1]

In this work we present an empirical shell model analysis of rms charge radii and E0 transitions for all nuclei in the region $16 \leq A \leq 40$ using the sd shell wave functions of Chung and Wildenthal.[2]

The charge radii $\langle R^2 \rangle_A$ are related to the experimental rms charge radii $\langle r^2 \rangle_A^{1/2}$ by

$$\langle R^2 \rangle_A = Z(\langle r^2 \rangle_A - \langle r^2 \rangle_{proton}) \qquad (1)$$

where $\langle r^2 \rangle_{proton}$ is the correction for the proton finite size.

The theoretical $\langle R^2 \rangle$ are given by

$$(\langle R^2 \rangle_{16_O} + \sum_j \alpha_j \langle j|r^2|j\rangle_p + \sum_j \beta_j \langle j|r^2|j\rangle_n - 2.4)(A/16)^{\lambda/3} \qquad (2)$$

where the coefficients α_j and β_j are the orbit occupations given by the sd wave functions; $\sum_j \alpha_j = Z-8$ and $\sum_j \beta_j = N-8$. The neutron matrix elements $\langle r^2 \rangle_n$ are only involved if they have an effective charge.[1] 2.4 fm^2 is the correction for center of mass motion. λ is a scaling parameter which has been discussed in another section of this report:

$$\lambda = 0.70(A-16)/24 \qquad (3)$$

The E0 matrix elements are related to the same single-particle $\langle r^2 \rangle$ matrix elements by

$$M(E0) = (\sum_j \gamma_j \langle j|r^2|j\rangle_p + \sum_j \delta_j \langle j|r^2|j\rangle_n)(A/16)^{\lambda/3} \qquad (4)$$

where γ and δ are coefficients obtained from the shell model wave functions; $\sum_j \gamma_j = \sum_j \delta_j = 0$.

The experimental data for $\langle R^2 \rangle_A$ and M(E0) are taken together with Eq. 2 and 4 to determine in a χ^2 search the best values of various combinations of the six parameters $\langle j|r^2|j\rangle$.

At first we make the usual assumption that only proton matrix elements contribute. The $\langle R^2 \rangle$ can be fit very well with one parameter. $\langle sd|r^2|sd\rangle = 10.9$ fm^2 except for the nuclei with A<23 for which the valence particle binding energies are small. ($\chi^2 = 0.8$ excluding A<23). If all three single-particle $\langle r^2 \rangle$ are allowed to vary independently the fit does not improve but indicates that the $d_{5/2}$ and $d_{3/2} \langle r^2 \rangle$ are the same whereas the $S_{1/2} \langle r^2 \rangle$ is slightly larger but not as well determined by the $\langle R^2 \rangle$ alone; $\langle s_{1/2}|r^2|s_{1/2}\rangle = 13.5 \pm 2.1$ fm^2. The fact that $\langle r^2 \rangle$ are the same for $d_{3/2}$ and $d_{5/2}$ is a consequence of the particular scaling relation (Eq. 3) chosen for λ.

The E0 transitions are very sensitive to the difference in the single-particle $\langle r^2 \rangle$ values since they must vanish if all $\langle r^2 \rangle$ are equal. The E0 transitions considered are given in Table I. Admixtures from the 0p and 0p-1f shells can also contribute to the low lying E0 transitions. In order to exclude these as much as possible we consider only the first excited 0^+ states from A=24-36 in the middle of the sd shell whose excitation energies are in fair agreement with the shell model calculation. Whether or not the E0 strength comes mainly from the sd shell wave functions might be tested in the future by calculating the (α,α') and (e,e') angular distributions.

The following results were obtained by a simultaneous fit to $\langle R^2 \rangle$ radii and E0 transitions.

All E0 transitions cannot be fit with a single set of $\langle r^2 \rangle$ values, instead we find two regions one (I) with A=24-30 which is best fit by a large difference

$$|\langle s_{1/2}|r^2|s_{1/2}\rangle_p - \langle d|r^2|d\rangle_p| \simeq 11 \text{ fm}^2$$

($\chi^2 = 2.0$ if s>d and $\chi^2 = 4.2$ if s<d) and another (II) with A=32-36 which is best fit with a smaller difference

$$|\langle s_{1/2}|r^2|s_{1/2}\rangle_p - \langle d|r^2|d\rangle_p| = 3.2 \text{ fm}^2.$$

($\chi^2 = 1.3$ if s>d and $\chi^2 = 2.0$ if s<d). In both cases the reduced χ^2 values favor $\langle s_{1/2}|r^2|s_{1/2}\rangle_p > \langle d|r^2|d\rangle_p$. The comparison with I and II is given in the Table.

Part of this large enhancement for the $s_{1/2}$ orbital at least in the lower part of the shell is probably explained by the large $\langle r^2 \rangle$ values obtained with Woods-Saxon wave functions for A=17.[3] However, Woods-Saxon calculations for A=39 give almost identical $s_{1/2}$ and d $\langle r^2 \rangle$ values. Hence the 30% enhancement for A≃34 remains to be explained. This discrepancy may be due to E0 core polarization, which has been calculated by Sharp and Zamick[1] to be large for A=17 using a Skyrme interaction. It would be interesting to have a calculation for the E0 core-polarization for nuclei near ^{40}Ca. These calculations indicate that the valence neutrons may also have an effective charge which is an effect similar to the well known E2 neutron effective charge.[3] However, fits with Eqs. 2 and 4 to the $\langle R^2 \rangle$ radii and E0 transitions result in a nearly vanishing neutron matrix element for the $s_{1/2}$ orbital,

$\langle s_{1/2}|r^2|s_{1/2}\rangle_n \sim 0.3 \pm 0.5$ fm^2.

1. R.W. Sharp and L. Zamick, Nucl. Phys. A208, 130(1973).
2. W. Chung, and B.H. Wildenthal, to be published.
3. B.A. Brown, A. Arima and J.B. McGrory, Nucl. Phys. A277, 77(1977).

TABLE I.--Comparison of experimental and theoretical E0 transition strengths. *indicates data not included in the fits.

Nucleus	E_x(MeV) Exp	Th	|M(E0)|(fm^2) Exp	Refs	Th(I)	Th(II)
^{18}O	3.63	4.02	6.0±0.7	a	0*	0*
	5.33	14.38	$\leq$4.5	a	0*	0*
^{20}Ne	6.72	6.24			6.0	1.7
^{22}Ne	6.24	5.77			4.0	1.1
^{24}Mg	6.43	7.42	6.3±0.3	b	5.7	1.6*
^{26}Mg	3.59	4.09	4.2±0.5	d	1.4*	0.4*
	4.97	5.24	3.3±0.2	d	5.9*	1.6*
	6.26	6.69	$2.1^{+1.8}_{-1.1}$	d	2.5*	0.7*
^{28}Si	4.98	5.20	6.8±0.4	b	7.2	2.0*
^{30}Si	3.79	4.08	1.44±0.10	c	1.5	0.4*
^{32}S	3.78	3.83	2.2±0.3	b	6.5*	1.8
^{34}S	3.91	4.09	1.55±0.15	c	6.2*	1.8
^{36}S	3.35	4.50	1.38±0.03	e	4.9*	1.4
^{36}Ar	4.33	4.63			5.0	1.4
^{38}Ar	3.38	5.83	2.3±0.2	c	3.9*	1.1*

[a] K.H. Souw, J.C. Adloff, D. Disdier and P. Chevallier, Phys. Rev. C11, 1899(1975).
[b] J.C. Adloff, K.H. Souw, D. Disdier and P. Chevallier, Phys. Rev. C11, 738(1975).
[c] K.H. Souw, J.C. Adloff, D. Disdier and P. Chevallier, Phys. Rev. C12, 1103(1975).
[d] F.W. Lees, A. Johnstone, S.W. Brian, C.S. Curran, W.A. Gillespie and R.P. Singhal, J. Phys. A7, 936(1974).
[e] J.C. Adloff, K.H. Souw, D. Disdier, F. Scheibling, P. Chevallier, W. Wolfson, Phys. Rev. C10, 1919(1974).

Evidence for Simple Shell Structure Effects in the Mass Dependence of $\hbar\omega$

B.A. Brown

One of the earliest observations on the properties of nuclei was that the root-mean-square (rms) charge radii have an average mass dependence from A=4-300 proportional to $A^{1/3}$. This is the result one would obtain from the hard packing of spheres and is a manifestation of the short-range repulsion in the nucleon-nucleon interaction. If the harmonic oscillator potential is used to generate a set of single particle orbitals which are filled as nucleons are added, one quickly finds that for large A the rms radii increase only as $A^{1/6}$. To compensate for this deficiency the harmonic oscillator parameter $\hbar\omega$ must be made mass dependent. Since the rms radii$\sim 1/\sqrt{\hbar\omega}$, $\hbar\omega$ must be $\sim A^{-1/3}$ and the best overall value is well known to be $\hbar\omega \approx 41\ A^{-1/3}$MeV.

In the present work we study the behavior of $\hbar\omega$ within a major oscillator shell and find that the mass dependence is very different from the overall average of $A^{-1/3}$.

From the experimental rms charge radii $\langle r^2\rangle_A^{1/2}$ we define a related quantity $\langle R^2\rangle$ by:

$$\langle R^2\rangle_A = Z(\langle r^2\rangle_A - \langle r^2\rangle_{proton}) \qquad (1)$$

where $\langle r^2\rangle_{proton}$ is the correction for the proton finite size.

The nuclei in the 1s-0d shell with a closed ^{16}O core and in the 1p-0f shell with a closed ^{40}Ca core will be considered. The only assumption in the model is that all of the nucleons in a given nucleus move in the same self-consistent average field characterized by a harmonic oscillator potential. The $\langle R^2\rangle$ values in the sd shell are given by

$$\langle R^2\rangle_A = (\langle R^2\rangle_{^{16}O} + (Z-8)\langle sd|r^2|sd\rangle - 2.4)(\tfrac{A}{16})^{\lambda/3} \qquad (2)$$

where $\langle sd|r^2|sd\rangle = \frac{7}{36}\langle R^2\rangle_{^{16}O}$

where λ is a scaling parameter; $\hbar\omega = \hbar\omega_o\ (A/16)^{-\lambda/3}$; conventionally $\lambda \approx 1$. 2.4 fm^2 is the small correction for center of mass motion.

Using the experimental data for $\langle R^2\rangle$ a value of λ can be extracted for each nucleus. The plot of λ vs. A in the sd shell is shown in Fig. 1. The experimental data from electron scattering experiments are from refs. 2-4; most points with small error bars are from model-independent analyses by Sick.[2] The trend in Fig. 1 strongly indicates a nearly linear mass dependence in λ which goes through zero at A=16. The points for A=19-22 are exceptions which are probably due to the small binding energy of valence proton particles at the beginning of the sd shell. The extrapolation to zero is supported by the nearly identical rms charge radii measured for the various oxygen isotopes which do not have the problem with valence protons. Thus almost all data in sd shell is in agreement with the linear expression:

$$\lambda(\text{sd relative to } ^{16}O) = 0.70\ (A-16)/24$$

For the fp shell nuclei Eq.2 becomes

$$\langle R^2\rangle_A = (\langle R^2\rangle_{^{40}Ca} + (Z-20)\langle fp|r^2|fp\rangle - 2.9)(\tfrac{A}{40})^{\lambda/3} \qquad (3)$$

where $\langle fp|r^2|fp\rangle = \frac{3}{40}\langle R^2\rangle_{^{40}Ca}$

λ vs. A is shown in Fig. 2; again nearly a linear A dependence is indicated by the data. The error bars represent the results of the most recent experiments listed in Ref. 3 (dashed lines connect an isotopic series measured by the same experimental group). However, the most recent rms values often differ by many standard deviations from earlier work and none of the fp shell rms values were obtained model independently. Thus, some of the deviation from a linear dependence in Fig. 2 may be due to systematic experimental errors.

Two lines are suggested by the data in Fig. 2:

$$\lambda(\text{fp relative to } ^{40}Ca) = (A-40)/40$$

and

$$\lambda(\text{fp relative to } ^{40}Ca) = 0 \qquad A \leq 48$$
$$= 1.1(A-48)/32 \qquad A \geq 48$$

Nuclei beyond ^{70}Zn for which rms radii have been measured, already have components from the 0g-1d-2s shell. However if the data in Fig. 2 is extrapolated to a hypothetical closed fp shell nucleus with A=80, at this point $\lambda \approx 1$ in agreement with the conventional average (the sd shell maximum was $\lambda \approx 0.7$).

It would be interesting to understand this behavior of λ. The sd shell Hartree-Fock calculations of Lee and Cusson[5] do not give this behavior but instead agree better with λ=1. The explanation is again probably associated with the restrictions on the nuclear density due to the hard-core repulsion. At the beginning of the sd shell the 0d orbit is being filled which contributes to the density mainly at the nuclear surface, the interior density does not increase significantly until the 1s orbit starts to fill toward the middle of the sd shell. The empirical mass dependence of λ suggests that the interior density is the most important factor.

1. L.J. Tassie and F.C. Barker, Phys. Rev. 111, 940(1958).
2. J. Sick, private communication.
3. C.W. DeJager et al., Atomic and Nucl. Data Tables 14, 479(1974).
4. H. Euteneuer et al., preprint; J.M. Finn et al., reprint.
5. H.C. Lee and R.Y. Cusson, Annals of Physics 72, 353(1972).

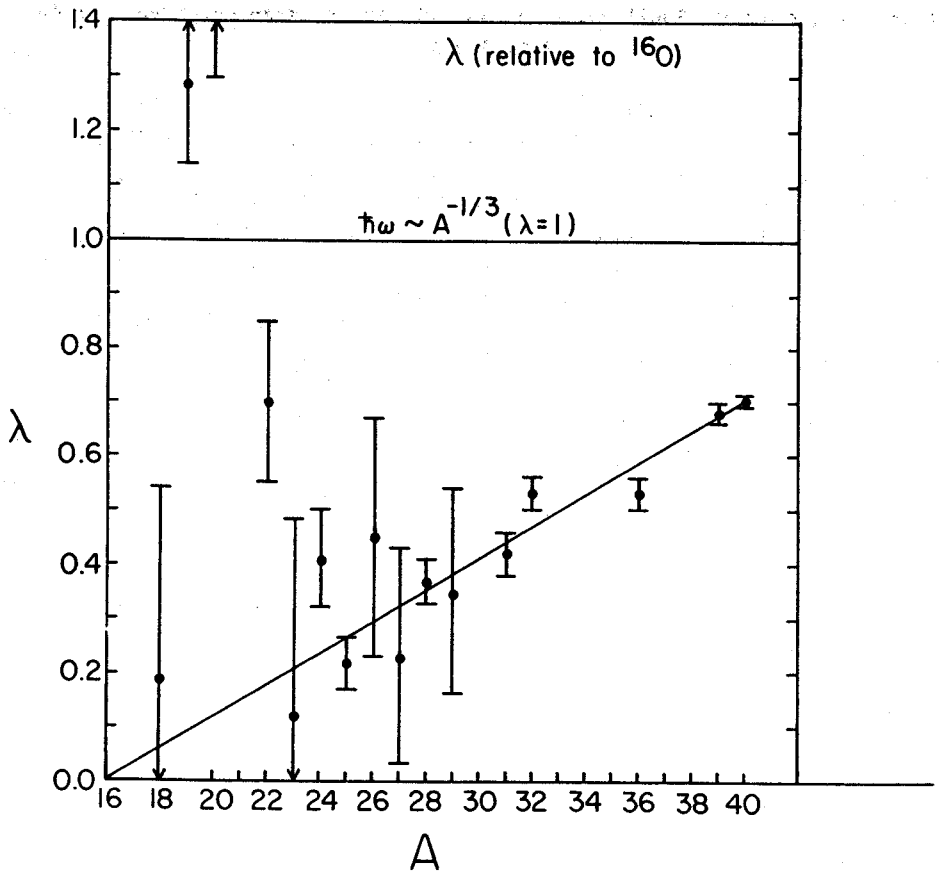
λ (relative to ^{16}O)
$\hbar\omega \sim A^{-1/3}$ (λ=1)
λ
A
1.4
1.2
1.0
0.8
0.6
0.4
0.2
0.0
16 18 20 22 24 26 28 30 32 34 36 38 40

FIG 1

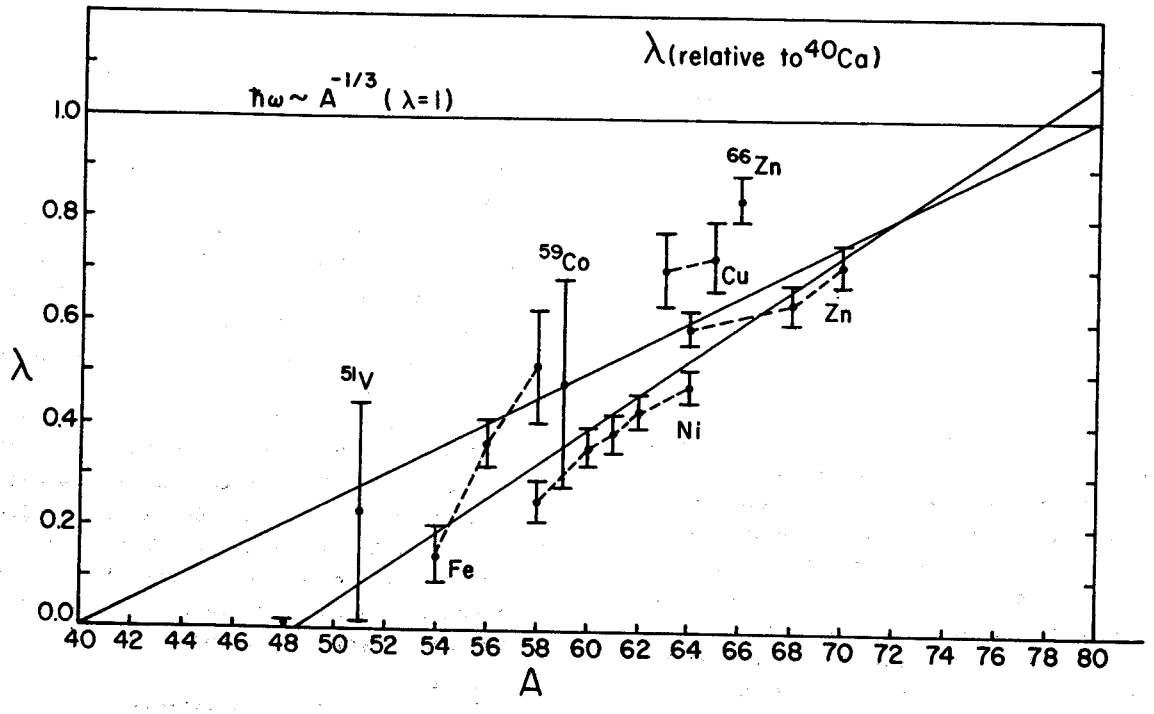
λ(relative to ^{40}Ca)
$\hbar\omega \sim A^{-1/3}$ (λ=1)
λ
A
^{66}Zn
^{59}Co
Cu
Zn
^{51}V
Ni
Fe
1.0
0.8
0.6
0.4
0.2
0.0
40 42 44 46 48 50 52 54 56 58 60 62 64 66 68 70 72 74 76 78 80

FIG 2